# Experimental Infection of Domestic Cats with Feline Herpesvirus-1 Strain CH-B Isolated from British Shorthair Cat

**Jiangting Niu**
Jilin agricultural university
**Han Zhao**
Jilin agricultural university
**Shuang Zhang**
Jilin Agricultural University
**Yanbing Guo**
Jilin agricultural university
**Qian Zhang**
Jilin Agricultural University
**Di Bao**
Jilin Agricultural University
**Hao Dong**
Jilin Agricultural University
**Fanxing Meng**
Jilin Agricultural University
**Yanli Zhao**
Jilin Agricultural University
**Hailong Huang**
Jilin Agricultural University
**Junzheng Wang**
Jilin Agricultural University
**Kai Wang**
Jilin Agricultural University
**Guixue Hu** ( huguixue901103@126.com )
Jilin Agricultural University https://orcid.org/0000-0003-4666-2221
**Shu-Shuai Yi**
Changchun Veterinary Research institute

**Research article**

**Keywords:** Feline herpesvirus-1, Domestic cats, Virus isolation, Natural host model, Experimental infection

**Posted Date:** October 22nd, 2020

**DOI:** https://doi.org/10.21203/rs.3.rs-94561/v1

# Abstract

**Background:** Feline herpesvirus-1 (FHV-1) is a most common virus that cause viral rhinotracheitis and ocular diseases in domestic cats and wild felids. As other alpha-herpesviruses, acute FHV-1 infection is responsible for severe upper respiratory tract and ocular disease, followed by lifelong latency that persist the limited virus in sensory neuronal cells. While latency reactivation can result in recrudescence, leading sever ocular lesions. Hence, FHV-1 infection in cats can be considered as a good natural host model to study alpha-herpesvirus pathogenesis.

**Results:** In this study, the FHV-1 CH-B was isolated from nasal discharge collected from a British shorthair cat in China, and was further identified via transmission electron microscopy (TEM) observation, indirect immunofluorescence assay (IFA) and genome analysis. Experimental infection of domestic cats with different dose of isolate CH-B, ranging from $10^4$ to $10^7$ $TCID_{50}$, showed that cats inoculated with $10^5$ $TCID_{50}$ not only showed typical upper respiratory track and ocular symptoms, but also could copy the progress of disease development. Therefore, the FHV-1 infection model was established by intranasally inoculated with $10^5$ $TCID_{50}$ of FHV-1 isolate CH-B. Infected cats began to show clinical signs at days 5 post inoculated (dpi), developed severe upper respiratory tract and ocular symptoms at 10-15 dpi, began to recover at 20 dpi, and recovered almost completely by 25 dpi. During acute infection period, virus mainly replicates in turbinate, conjunctiva, cornea and sensory neuronal cells, while virus only persists in trigeminal ganglia (TG) at lifelong latency. Viremia and viral infections in lungs do not appear in FHV-1 CH-B infected cats, with only one exception. We also demonstrate that FHV-1 CH-B infection can induce severe inflammatory responses and lung, trachea, and tonsils tissues damage in cats. In addition, we found that FHV-1 infected cats can shed virus via nasal and ocular discharge, resulting FHV-1 infection in in-contact cats.

**Conclusions**: This natural host model of FHV-1 infection will be valuable for the screen and assessment of antiviral drugs and vaccines, as well as the studies of the pathogenesis of alpha-herpesvirus infection in animals and humans.


# Background

Feline viral rhinotracheitis (FVR), a most common and highly contagious upper respiratory track and ocular disease of felids, is caused by feline herpesvirus-1 (FHV-1) and seriously threatens the health of domestic cats and wild felids worldwide. FHV-1 is an enveloped double-stranded DNA (dsDNA) virus classified under the *Varicellovirus* genus within the *Alphaherpesvirinae* subfamily, with an approximately 134 kb genome [1]. FHV-1 displays the same replication characteristics, including a short replication cycle, lifelong latency primarily in neurons and a narrow host range, with many other alpha-herpesviruses [2]. Clinically, FHV-1 is responsible for approximately 50–75% of all diagnosed viral upper respiratory infections in domestic cats and is often fatal to 3-6-month-old kittens with the mortality rates of up to 50% [3]. Following exposure of the oronasal and conjunctival mucous membranes, FHV-1 primarily replicates in epithelial cells at these sets, resulting in fever, depression, pyrexia, anorexia, sneezing,

conjunctivitis, corneal ulceration, keratitis, and ocular and nasal discharge [4]. The acute phase of FHV-1 infection is followed by lifelong latency, a hallmark of many alpha-herpesviruses infections [5]. During the latent stage, viral DNA persist mainly in sensory ganglion neurons, including olfactory bulbs, optic nerve, optic chiasm and trigeminal ganglia (TG) [6, 7]. No infectious virus can be recovered from tissues because of the very limited transcription of viral RNA. However, the natural stressors or the administration of corticosteroids can induce the viral reactivation in latently infected cells, leading to renewed virus production and shedding of infectious virus [4, 6]. Reactivated infectious virus then travels to the periphery and can lead to ocular or nasal lesions, or lead to viral transmission.

Since the first FHV-1 strain was isolated from the trachea of sick kitten in America in 1958, infections of this virus in domestic cats have been reported in the majority of countries, including Germany, Japan, Australia, Canada, Hungary, the United Kingdom and China, with epidemic and widespread distribution worldwide [8]. Moreover, the prevalence of FHV-1 in wild felids, such as tigers, California mountain lions, jaguars, oncillas, cheetahs, and et al, increased gradually in the past few years [9–11]. Currently, limited FHV-1 vaccines are used to prevent FHV-1 infection, but these vaccines can not provide 100% of protection, especially for cats in FHV-1 lifelong latency. Clinically, supportive treatment and topically and systemically antiviral therapy are the most commonly used options for FHV-1 therapy [4, 6]. In recent years, many new vaccines and antiviral drugs against FHV-1 were designed and evaluated, and some antiviral drugs have shown the ability to inhibit the replication of FHV-1 in vitro [12, 13]. Further evaluation of these vaccines and drugs should be performed exclusively in domestic cats in preclinical and clinical trials. Thus, a scientific and convenient FHV-1 infection model in domestic cats is required for the assessment of novel immunization and treatment strategies. Furthermore, due to the same clinical and replication characteristics between FHV-1 and human herpes simplex viruses type 1 (HSV-1) and 2 (HSV-2), such as respiratory and ocular disease, lifelong latency and reactivation, FHV-1 infection in domestic cats can be considered to be an ideal infection model to study human herpesvirus.

In this study, we described the isolation of a virulent FHV-1 strain referred as CH-B from British shorthair cat in Northeast China, and confirmed the optimal experimental infectious dose in domestic cats by monitoring survival rate, clinical score and virus shedding. Finally, an FHV-1 infectious model was established using the optimal infectious dose, and the detailed infection data was also monitored.

# Results

### Virus isolation and identification

One FHV-1 strain, designated FHV-1 CH-B, was successfully isolated from a British shorthair cat. After purification, the stable CPE was observed when five additional continuous cultures, characterized by cell rounding, pyknosis and focal-like forms, eventually necrosis and shed completely (**Fig. 2a**). The supernatants of all five purified cell cultures were tested to be positive for FHV-1 using specific primers HerpF and HerpR targeting FHV-1 TK gene, and the nucleotide sequences of obtained 292-bp fragments showed 100% identity with that of FHV-1 reference strains. FHV-1 CH-B strain was further identified via

IFA using anti-FHV-1 antibody, bright green fluorescence was found in infected cells subject to fluorescence microscope, in contrast, no fluorescence was found in control cells (**Fig. 2a**). TEM of negatively stained isolate revealed spherical virus particles with a diameter of 140 nm, numerous spikes on the surface of envelope, which accord with the structural characteristics of herpesvirus (**Fig. 2b**).

## Genome analysis

The nearly complete genome sequences were successfully sequenced and deposited in GenBank under accession number MT813047. The genome of isolate CH-B was 134,779 bp in length and contained 76 open reading frames (ORFs). We predicted and verified that the genomic organization of isolate CH-B was identical to other FHV-1 reference stains previously described (data not shown). Comparative genomic analysis showed that the higher nucleotide identities were found between the isolate CH-B and FHV-1 reference sequences retired from GenBank, with a mean value of 98.14% (97.7% -98.8%). A neighbor-joining (NJ) tree including canine herpesvirus type 1 (CHV-1) as an outgroup was generated based on the complete genome nucleotide sequences (**Fig. 3**), and showed that the isolate CH-B was more closely related to FHV-1 reference strains and form a group distinct from CHV-1. Moreover, the NJ tree suggested that FHV-1 clusters primarily correlated with geographic location.

## Optimal infectious dose

To determine the optimal infectious dose of FHV-1 CH-B strain, domestic cats were inoculated intranasally with different doses of viruses, and were evaluated via various indicators. Cats in group A ($10^7$ $TCID_{50}$), group B ($10^6$ $TCID_{50}$) and group C ($10^5$ $TCID_{50}$) showed initial clinical signs at days 2, 4 and 5 post inoculation (dpi), respectively, accompanied by an increase of rectal temperature (>103°F) and significant weight loss (**Fig. 4ab**). These cats presented with nasal serous secretion, sneezing, dyspnoea and anorexia. Subsequently, the tested cats showed more severe clinical signs gradually, which manifested on increasing palpebral and nasal purulent secretion, symblepharon and skin ulcers of the nose. As the disease progressed, the clinical scores were more than 5, and cats in group A, B and C began to die at 6, 10 and 14 dpi, respectively (**Fig. 4c**). While no clinical sign was observed within cats in group D ($10^4$ $TCID_{50}$) except for mild anorexia at 7 dpi. At 15 dpi, the survival rates in group A, B, C, D and E were 0/4, 0/4, 3/4, 4/4 and 3/3 (**Fig. 4d**).

Nasal and conjunctival swabs were collected daily, and were used to test for FHV-1 shedding by PCR. The monitoring results (**Fig. 4e**) showed that FHV-1 shedding originally occurred in nasal cavity of infected cats, and then in eyes. Cats inoculated with different doses of FHV-1 showed different characteristics of viral shedding. Cats in group A, B and C began to release viruses via nasal or ocular discharge at 3 dpi, while viral shedding was detected at 7 dpi for cats in group D. Control cats in group E remained healthy throughout the trial.

From the above comparison and contrast, cats inoculated with excessive doses ($10^7$ $TCID_{50}$ and $10^6$ $TCID_{50}$) of FHV-1 CH-B strain showed acute infection and high mortality rate, while low-dose group ($10^4$ $TCID_{50}$) did not show distinct clinical signs, only released viruses. In contrast, cats inoculated with $10^5$ $TCID_{50}$ of CH-B strain not only showed typical upper respiratory track and ocular symptoms, but also could replicate the progress of disease development. So, we choose $10^5$ $TCID_{50}$ as the optimal infectious dose to develop FHV-1 experimental infection model.

## FHV-1 experimental infection model

*Clinical signs*

Domestic cats inoculated intranasally with the optimal infectious dose ($10^5$ $TCID_{50}$) of CH-B strain (Artificial inoculation group) replicated the disease progress of FVR, from acute infection phase to lifelong latency. Artificial inoculated (AI) cats begin to sneeze and cough at 5 dpi, accompanied by depression and anorexia. With the progression of disease, AI cats showed typical clinical symptoms of FVR (at 10 dpi), including fever, dyspnea, serous or purulent discharge in nasal cavity and eyes, and nasal skin ulcer, followed by deterioration (at 13 dpi) and death (**Fig. 5a**). Oculonasal purulent discharge and other clinical signs of most of survivors decreases and disappear at 20 dpi, and almost fully recovering at the end of study. Notably, clinical signs for most of cohabiting cats initially appeared at 10 dpi, and peaked at 16 dpi. The changes of clinical score, rectal temperature and body weight were showed in **Fig 5bcd**. At the peak of disease, the clinical score was >5, for AI cats, the rectal temperature was more than 103°F, and the weight loss rate was >4%. The survival rates in three groups were 9/15, 7/9 and 9/9 at the end of study (**Fig. 5e)**.

*Antibody responses to FHV-1 infection*

Before starting the experiment (5 days prior to inoculation), all cats were negative for anti-FHV-1 antibodies based on the negative ELISA results. All serum samples from CH-B challenged cats (Artificial inoculation group) showed a positive reaction with very low antibody titers in the ELISA at 5 dpi, and peaked at 15 dpi (**Fig. 6)**. For cohabitation infected cats, the anti-FHV-1 antibodies were not detected by ELISA or very low until 10 dpi, and then increased rapidly by 20 dpi. All the surviving cats in these two groups remained seropositive until the end of the experiment. Furthermore, all mock-inoculated cats (negative control) were serologically negative for FHV-1 throughout the study.

*Inflammatory responses to FHV-1 infection*

The white blood cells (WBC) in AI cats significantly rose compared with control cats at 5, 10 and 15 dpi, although the WBC in most of AI cats did not exceed the upper limits of normal (ULN) (**Fig. 7b)**. There was a significant increase in blood lymphocyte (LYM) in AI cats at 15, 20 and 25 dpi, compared with controls (**Fig. 7c)**. Furthermore, from 5 to 20 dpi, serum SAA contents in AI cats exceed the ULN, and were

significantly higher than that in controls (**Fig. 7a)**. For cohabiting cats, the significant increases of WBC and SAA were observed from 10 to 25 dpi, and no significant change in LYM appeared.

*Virologic responses*

We examined virus shedding and viral titres in all cats by collecting nasal and ocular swabs at each time point. As shown in **Fig. 8**, virus shedding in nasal cavity were detectable in 8 of 15 AI cats at 1 dpi by quantitative PCR, and in all AI cats at 3-21 dpi. Viral DNA copies in nasal swabs maintained in a higher level (ranging from $10^{5.68}$ copies/ml to $10^{6.51}$ copies/ml) at 3-15 dpi, while decreased rapidly after 17 dpi. Viral DNA was detected in unilateral ocular swabs collected from a few AI cats at 3 dpi, and in ambilateral eyes of all AI cats from 7 to 21 dpi, with the viral loads (ranging from $10^{5.91}$ copies/ml to $10^{6.66}$ copies/ml) peaking between 9-15 dpi. Furthermore, AI cats released more virion through eyes at acute infection period (9-15 dpi). No detectable viral DNA was found in nasal cavity and eyes of all AI cats from 23 to 25 dpi, except one cat with low viral loads of $10^{2.17}$ copies/ml in left eye at 23 dpi.

We also examined viraemia and viral replication in the primary tissues (**Fig. 9**), including turbinate, conjunctiva, cornea, trigeminal ganglia (TG), ciliary ganglia (CCG), optic nerve, olfactory bulb, trachea, tonsils, lung, liver, kidney, spleen and intestine. Viral loads were detectable at 5, 10, 13 (dead of infection) and 15 dpi in turbinate, conjunctiva, cornea, TG, CCG, optic nerve and olfactory bulb of all AI cats, and viral DNA copies reached peaks at 13 dpi. Furthermore, we only detected viral loads in trachea ($10^{3.28}$ copies/ml) and tonsils ($10^{2.35}$ copies/ml) collected from three cats died on 13 dpi. Only one cat died on 13 dpi showed detectable viral DNA in lung. Other tissues were tested to be negative for FHV-1 at each time point. Viral DNA were still detected in TG of all AI cats at 25 dpi with a mean viral load of $10^{2.27}$ copies/ml, while no viral DNA was detected in other tissues at 25 dpi with very few exceptions.

For in-contacted cats, viral DNA were detectable in nasal cavity and eyes from 7 to 19 dpi, the change of viral loads coincided with AI cats (**Fig. S1**). Same as AI cats, viral loads were detectable in turbinate, conjunctiva, cornea, TG, CCG, optic nerve, olfactory bulb, trachea and tonsils, but not in lung and other tissues (**Table S2**). No viral DNA were detected in all swabs and tissues from all uninfected control cats.

*Pathology and histopathology*

Cats died of infection and euthanized cats were dissected according to the standard operational procedures, subjected to pathological and histopathological examinations. No tissue lesion was observed in any of cats at 5 dpi. Compared with control cats, AI cats at 10 dpi displayed mild lesions, including lung congestion and tracheal mucous secretions. Severe tissue lesions, including multifocal necrosis throughout the lung, dark-reddish purulent secretions in trachea, and tonsils severe congestion and necrosis, were observed in AI cats at 13 or 15 dpi (**Fig. 10**). The obvious lesions were not observed in other tissues. Histopathological examination at 13 dpi showed that strain CH-B caused coalescing severe interstitial pneumonia with diffuse lesions, characterized by destroyed alveoli, thickened alveolar septa accompanied with infiltration of inflammatory cells (including macrophages and lymphocytes), and

aggregation of inflammatory cells in partial alveolar cavities (**Fig. 10c**). More seriously, the destruction of alveoli was observed microscopically in 30%-50% of the lung tissue. Alveolar wall dissolves, and adjacent alveoli fuse to form a large cavity accompanied with infiltration of inflammatory cells and fibrin exudation. Microscopically, the thickened mucous layer accompanied with infiltration of macrophages and lymphocytes, and hyperaemia and haemorrhage were observed in diseased trachea of AI cats (**Fig. 10b**). Furthermore, in necrotic tonsil of AI cats, there were large amounts of inflammatory cells (**Fig. 10a**). The lung and trachea from cohabiting cats at 15 and 18 dpi displayed moderate interstitial pneumonia and tracheitis (data not shown). Immunohistochemistry (IHC) examination showed that viral antigens for FHV-1 were found in alveolar epithelia and tracheal epithelial cells in areas of lung and trachea lesions from AI cats and cohabiting cats (**Fig. 10d**). The mock-infected cats showed no histopathological change and viral antigen.

# Discussion

Upper respiratory tract disease (URTD) caused by numerous pathogens, including bacteria, mycoplasmas, chlamydiae and viruses, is most common clinical disease in felids [14]. Thereinto, FHV-1 is an important and common viral pathogen of cats and is also responsible for 20%-50% clinical case of feline URTD [15]. FHV-1 mainly cause URTD and ocular disease after infection by oral, nasal or conjunctival route, and often do not cause viremia and serious systemic infections, resulting a high morbidity, but a low mortality for domestic cats [6]. Although widespread vaccination had reduced the morbidity associated with FHV-1 in cats, FHV-1 carriers are still prevalent because of the characteristics of lifelong latency. Here, a field FHV-1 strain was isolated from a British shorthair cat seeking medical attention, and was further confirmed through viral isolation, IFA, TEM examination, PCR identification, genome sequence, and phylogenetic analysis. This filed isolate finally named FHV-1 CH-B. Phylogenetic analysis showed that isolate CH-B shared 97.7%-98.8% nucleotide identities with FHV-1 reference strains based on the complete genome sequence, and grouped within the same group compared to CHV-1. Interestingly, FHV-1 strains isolated from different geographic location gathered in different clusters, in accord with previously described by Andrew, et al. [16]. Furthermore, preliminary animal challenge experiment demonstrated that FHV-1 CH-B strain was virulent in cats, and could cause typical clinical symptoms of FVR, including sneezing, conjunctivitis, and ocular and nasal discharge.

At present, there were triple inactivated or attenuated vaccine against FHV-1, feline calicivirus (FCV) and feline panleukopenia virus (FPV) for the prevention of FHV-1, but these vaccines do not provide the complete protection for immunized cats [3]. L-lysine, omega-interferon (IFN-ω), corticosteroids, and DNA analogues (such as Ganciclovir, Cidofovir, Famciclovir and Aciclovir, et al.) have been widely used in the topical or systemic antiviral therapy for FHV-1 infections [12, 13, 17], however, they seem ineffective for severe infections. Vaccine development and screening of new antiviral drugs are essential for the prevention and treatment of FVR. In additional, the mechanisms of lifelong latency and secondary incidence for FHV-1 are still unclear. Therefore, developing an FHV-1 infection model in domestic cats that simulate the process of acute infection-lifelong latency for FHV-1 will be highly beneficial, as it not only can be used to study FHV-1 pathogenesis, but also plays an important role in preclinical evaluation

of vaccine and antiviral drugs against FHV-1. Several FHV-1 challenge experimentations have been described in previous studies, but the systemic evaluation is absent [18, 19]. In the present study, an FHV-1 infection model in domestic cats was established using isolate CH-B, and was scientifically assessed by detecting the clinical, virologic, inflammatory and antibody responses targeting FHV-1 infection.

Firstly, the optimal infectious dose of isolate CH-B in cats was determined, as the too high or too low infectious dose is adverse to fully copy the process of acute infection-lifelong latency for FHV-1. Our experimental results reveal that the infectious dose of $10^4$-$10^7$ $TCID_{50}$ can cause the different degrees of upper respiratory tract infection and ocular disease. Cough and sneezing are the major clinical feature in the early stage of infection. In acute infection period, infected cats displayed severe nasal and ocular signs, mainly mucinous or purulent discharge, some seriously infected cats finally died because of dehydration and respiratory failure [4, 6]. Moreover, viral shedding was observed at 3 dpi for cats inoculated $10^7$, $10^6$ and $10^5$ $TCID_{50}$ of CH-B, while was observed at 7 dpi for cats inoculated $10^4$ $TCID_{50}$, suggesting that the severity of FHV-1 infection is associate with the infectious dose. Interestingly, viral shedding was observed firstly in nasal discharge and then in ocular discharge, however, the ocular signs seemed more severe in acute infection period. Hamano et al. described the same clinical features in cats infected with isolate C7301, while the severe ocular clinical manifestations were rarely reported in other experimentally infected cats [19]. This may be related to the pathogenicity of FHV-1 isolates. Furthermore, the lifelong latency was not evaluated in this experimental phase, but we found some cats infected with $10^5$ $TCID_{50}$ of isolate CH-B markedly improved after 13 dpi. This is also one of the reasons why we choose $10^5$ $TCID_{50}$ ass the optimal infectious dose.

As expected, we copied the process of acute infection-lifelong latency for FHV-1 by intranasal $10^5$ $TCID_{50}$ of FHV-1 isolate CH-B inoculation. Cats inoculated with isolate CH-B began to show clinical signs (cough and sneezing) at 5 dpi, developed severe upper respiratory tract and ocular symptoms at 10–15 dpi, began to recover at 20 dpi, and recovered almost completely by the end of the study. The change of rectal temperature, body weight loss rate and clinical score are almost consistent with the progress of FHV-1 infection. It has been reported that FVR has an incubation period of 2 to 6 days after exposure of FHV-1 in the nasal cavity or conjunctiva, and clinical signs usually subside within 10–20 days post infected [6, 7]. Clinical data from this study further offer evidences for the study of FVR. Virus shedding was first detected in nasal swabs at 1 dpi, and continued to be detected until 19 dpi. However, during the early stages of infection, virus shedding was first detected in unilateral ocular swabs from eyes with clinical signs at 3 dpi. Interestingly, viral titres in ocular swabs were higher than that in nasal swabs during acute infection stage. Based on current knowledge, we suggest that nasal swabs are the preferred diagnostic sample for confirmation of FHV-1 infection during the early stages of infection, but ocular swabs should be preferred during the acute infection stage. Virus titres in nasal and ocular swabs of cats inoculated with isolate CH-B increased rapidly after 3 dpi, peaked on 7–15 dpi, and decreased promptly after 17 dpi. However, the antibodies against FHV-1 were very low until 5 dpi, and then increased rapidly by 15 dpi. It suggested that the virus clearance occurred rapidly in all infected cats by the production of anti-FHV-1 antibody during acute infection stage. The detection of viral DNA distribution in the tissues showed that

viral DNA were detectable in turbinate, conjunctiva, cornea, TG, CCG, optic nerve and olfactory bulb during the early stages of infection and acute infection stages (5–15 dpi), and viral titres reached peaks at acute infection stages. However, viral loads were not detectable or very low at 25 dpi in all tissues, except TG, suggesting FHV-1 CH-B establish latent infection at 25 dpi. Previous studies had demonstrated that FHV-1 primarily replicates in nasal mucous, turbinate, conjunctiva and cornea during acute infection period, resulting upper respiratory tract and ocular diseases, while persists in sensory ganglion neurons, mainly in TG and optic nerve, during the latent stage [20]. Viremia and viral infections in lungs were rare in clinical cases of FHV-1 infection. Based on animal challenge experiment, viral DNA were also detected in trachea, tonsils and lung from cats died due to infection at 13 dpi, but not detected in these tissues at other time point, suggesting that it is difficult to cause viremia and viral infections in lungs for FHV-1 CH-B infection. Furthermore, we also analysis the inflammatory responses against FHV-1 infection by detecting complete blood count and serum SAA level, and found that WBC, LYM and SAA increase significantly after FHV-1 infection, although the counts of WBC and LYM of most infected cats do not exceed ULN. SAA, as a typical acute-phase protein, is a sensitive indicator to evaluate the infection of virus and bacteria and inflammatory responses [21]. We found that serum SAA increased rapidly after FHV-1 infection and reached a very high level at 15–20 times the normal during acute infection period, while recovered normally at 25 dpi. It suggested that FHV-1 infection can cause severe inflammatory responses in cats. Histopathological examination also demonstrate that FHV-1 infection can induce inflammatory responses in trachea, lungs and tonsils. Furthermore, cohabitation infection tests demonstrate that domestic cats can infect FHV-1 by touching FHV-1 infected cats, and show the same clinical signs, virologic, antibody and inflammatory responses with artificially inoculated cats.

Most of alpha-herpesviruses, such as HSV-1, canid herpesvirus 1 (CHV-1) and FHV-1, commonly infect and can cause upper respiratory tract and ocular disease, and can established latent infection by hiding viruses in sensory neurons of the peripheral nervous system [2, 22]. Following reactivation, virus will replicate again in nasal cavity and eyes, leading recurrent ocular disease, even leading to blindness. Due to the striking similarities in pathogenesis of HSV-1, CHV-1 and FHV-1, FHV-1 infection in cats or CHV-1 infection in dogs are proposed as valuable natural host models to study human herpesvirus pathogenesis, and to screen novel vaccines and antiviral drugs [22]. In the present study, FHV-1 CH-B infection can recreate the typical characteristics of the ocular disease, including relevant virologic, immune and inflammatory responses, and can also recreate acute and latent infection. Therefore, FHV-1 CH-B infection model established in this study can be proposed to be a good representation of herpesvirus ocular infections to develop more effective immunization and treatment procedures against alpha-herpesvirus infection in animals and humans.

# Conclusion

An FHV-1 isolate CH-B was obtained from a British shorthair cat, and an experimental infection model was established by determining the optimal infectious dose and evaluating clinical signs, and virologic, immune and inflammatory responses in the present study. We demonstrate that FHV-1 CH-B can induce the typical clinical features of FVR, and establish latent infection by hiding viruses in TG. We also showed

that FHV-1 infected cats can shed virus via nasal and ocular discharge, resulting FHV-1 infection in in-contact cats. Our natural host model of FHV-1 infection will be valuable for the screen and assessment of antiviral drugs and vaccines, as well as the studies of the pathogenesis of alpha-herpesvirus infections in animals and humans.

# Methods

### Ethics statement

All animal experiments in the present study were performed with the approval from the Animal care committee of Jilin Agricultural University.

### Clinical samples

A total of 17 nasal swaps were collected from suspicious FHV-1-infected cats, which exhibited fever, sneezing, conjunctivitis, and oculonasal discharge, in animal hospital of Jilin agricultural university between December 2016 and May 2017. Samples were tested using a PCR assay against FHV-1 described previously by Sykes et al [23]. FHV-1-positive samples were dissolved in 1 ml of minimum essential medium (MEM) containing 100 U/ml penicillin-streptomycin and then homogenized in a vortex. Then, the supernatant was collected after centrifuged at 8000×g for 5 min, and was filter-sterilized via 0.22 μm filtering films, subject to the isolation of FHV-1. The filtrates were stored at -80 ℃ until further use.

### Virus isolation and purification

Feline kidney 81 (F81) cell monolayers in 25 $cm^2$ culture flasks was inoculated with 500 μl of the filtered supernatants from FHV-1-positive samples, and cultured at 37 ℃ in a 5% $CO_2$ incubator. The cytopathic effect (CPE) was monitored every 12 h. If no CPE was observed until the fourth day, the cell cultures were freeze-thawed and further inoculated into the F81 monolayers. Each positive sample was passaged five times, the cultures were freeze-thawed to release virus when 80% CPE appeared. The harvested viruses were purified by a plaque assay as described previously [24]. Then, the purified viruses were passaged continuously until the CPE and viral titres were stable. The viral titres were calculated using the Reed-Muench formula and expressed in the median tissue culture infective dose $\log_{10}$ ($TCID_{50}$/ml).

### Virus identification, genome sequencing and analysis

The purified virus was centrifuged at 30,000×g for 10 min, and then was negatively stained by 2% phosphotungstic acid for transmission electron microscopy (TEM) observation.

F81 monolayers cultured in 24-well microtitre plates were inoculated with the purified viruses, the multiplicity of infection (MOI) was 0.01, and then cultured until 50% CPE appeared. The cell cultures were fixed in 80% ice cold acetone for 20 minutes, and washed three times using phosphate-buffered saline (PBS). Then, fluorescence staining was performed using an FHV-1 indirect immunofluorescence kit

(VMRD, NewtherLand) according to the manufacturer's instruction. The specificity fluorescence was observed via immunofluorescence microscope, also compared to the normal cells at the same time.

Viral genome DNA was extracted from the cell cultures using AxyPrep$^{TM}$ Body Fluid Viral DNA/RNA Miniprep Kit (Axygen, China) according to the manufacturer's instructions, subjected to PCR identification and genome cloning and sequencing. The full-length genomes of FHV-1 isolates were amplified using 53 pairs of overlapped primers (primers sequences were shown in **Table S1**) designed according to FHV-1 reference strain C-27 (GenBank accession number FJ478159) in this study. The PCR products were cloned into PMD-18T vectors and positive clones were sent to Sangon Biotech (Shanghai, China) for Sanger sequencing. Cloning and sequencing were performed at least three times for each PCR fragment. The nucleotide sequences were assembled using Seqman program and multiple sequences alignment was performed with MAFFT (https://mafft.cbrc.jp/alignment/server/). Phylogenetic analyses were conducted using the neighbor-joining method, the Kimura 2-parameter model, and 500 bootstrap replicates in MEGA 7.0 software. Finally, the trees were visualized using Figtree v1.4.3.

## Experimental design

### *Animal*

Fifty-two 3-month-old cats (female:male=1.36:1) purchased from a pet market (Changchun, China) were used in this study. All cats were confirmed to be negative for the common pathogens of feline upper respiratory track disease (URTD), including FHV-1, feline calicivirus (FCV), Chlamydia felis (Cf), Bordetella bronchiseptica (Bb) and Mycoplasma felis (Mf), by PCR/RT-PCR, and were also free for FHV-1 antibodies as assessed by a FHV-1 antibody detection Kit (EVL, Holland). Each cat was housed in a separate cage, and each group was placed in individual containment room with the same condition. Prior to the study, all cats were acclimated for 7 days.

### *Optimal infectious dose*

Nineteen cats were randomly assigned into five groups. Groups A, B, C and D of four cats each were inoculated intranasally with 1 ml virus cultures/cat (0.5 ml for each nasal passage) containing $10^7$, $10^6$, $10^5$ or $10^4$ $TCID_{50}$ of FHV-1 CH-B strain (isolated in this study), respectively. Group E of three cats as control group was mock-inoculated with 1 ml of MEM by intranasal route. Each group was placed in separate containment room. Following viral inoculation, survival rates, rectal temperatures, clinical signs and scores were monitored daily. Nasal and conjunctival swabs were collected to determine virus shedding each day.

### *FHV-1 infection model*

FHV-1 infection model was established and the detailed infection data was also monitored based on the determined optimal infectious dose. Thirty-three cats were randomly divided into three groups. Artificial inoculation group (FHV-1 infection model) of 15 cats was inoculated with 1 ml $10^5$ $TCID_{50}$ of FHV-1 CH-B

strain (the optimal infectious dose) by intranasal route. Cohabitation infection group of nine cats was not inoculated, but kept in the same cage at a ratio of 1:1 with cats in artificial inoculation group in the same room, mimicking natural infection. The other 9 cats served as control, were mock-inoculated intranasally with 1 ml of MEM, and housed in the individual containment room. Rectal temperatures, survival rates, clinical signs and scores were monitored daily. Nasal and conjunctival swabs were collected to determine virus shedding and titers each day. Blood samples were collected from all cats on day 0, 3, 5, 10, 15, 20, 25, post-inoculation and were used for the evaluation of FHV-1 antibodies titers, serum amyloid A (SAA) and the complete blood count. Three artificial inoculation cats, two cohabitation infection cats and 2 controls were humanely euthanized with an intravenous injection of pentobarbital sodium according to the protocol suggested by World Society for the Protection of animals about Methods for the euthanasia of dogs and cats on day 5, 10, 15 and 25 post-inoculation, respectively (**Fig. 1**). Then, the lung, liver, kidney, spleen, intestine, tonsils, trachea, conjunctiva, cornea, TG, optic nerve, olfactory bulb and ciliary ganglia (CG) were collected using sterile technique for the analyses of virus tissue distribution, virus titers and histopathology.

## Clinical, laboratory and virologic assessments

*Clinical score*

All cats were observed daily by two experienced veterinarians at three different times. Taking rectal temperatures, physical condition, and respiratory track, ocular and oculonasal skin signs, clinical scores were assigned to each cat daily using a modified scoring system based on the USDA supplemental Assay Method 3111 as described previously [20].

*Detection of anti-FHV-1 antibodies*

Serum samples were screened for anti-FHV-1 antibodies using a indirect ELISA kit (EVL, Holland) following the manufacturer's instructions. Each serum sample was tested in duplicate wells. The OD450 values of the negative serum provided in the kit were used to determine cutoff values.

*2.6.3. Virus shedding and viral titers test*

All collected swabs and tissues were individually homogenized in 500 μl of PBS, after centrifuged at 8000×g for 5 min, the supernatant was used for the extraction of viral genome DNA. Virus shedding and virus tissue distribution were detected using a PCR assay described above. Viral titers were measured using a TB green-based real-time quantitative PCR (qPCR) assay developed in our laboratory. Briefly, qPCR was performed using TB GreenTM Fast qPCR mix (Takara, Japan) and one pair of primers (F: 5'-AGAAGGACAACTAGGGGAAAACAA-3'; R: 5'-GATAGCGGGACTTTACGGACATAC-3') targeted FHV-1 gB gene in ABI 7500 Fast Real-time PCR system (Invitrogen, USA) with the following reaction conditions: 94℃ for 10 min, followed by 40 cycles of 94℃ for 5 s and 60℃ for 30 s. The standard curve was plotted from the results of parallel PCRs performed on serial dilutions of standard gB-positive plasmid. Viral loads (copies/μl) in swabs and tissues were calculated by normalization to the standard curve.

*Histopathology and immunohistochemistry*

Tissue samples were fixed in 10% buffered formalin and embedded in paraffin wax. Some sections were stained with haematoxylin and eosin (HE) for histopathological assessment. Other tissue sections were used for immunohistochemistry (IHC) tests with anti-FHV-1 antibody (VMRD, USA) and HRP-labeled rabbit anti0feline secondary antibody (Gibco, USA).

*Complete blood count and SAA analysis*

Complete blood count and SAA protein were measured using a hematology analyzer (PE-6800VET, Prokan, China) and a VetTest plasma chemistry analyzer (IDEXX, USA), respectively, in animal hospital of Jilin agricultural university.

### Statistical Analysis

Rectal temperatures, clinical scores, viral titers, complete blood count and SAA levels were analyzed with the statistical program PASW statistics 19.0 (SPSS) and presented as mean±SEM. One-way ANOVA followed by Tukey's multiple comparison tests was used to compare the differences of various indicators among different groups. The significance of differences between two groups was analyzed using s Student's t-test. Probability ($p$) values <0.05 was considered as statistically significant.

## Abbreviations

FHV-1: Feline herpesvirus-1; FCV: Feline calicivirus; FPV: Feline panleukopenia virus; HSV-1: Herpes simplex viruses type 1; HSV-2: Herpes simplex viruses type 2; CHV-1: Canid herpesvirus-1; IFA: Indirect immunofluorescence assay; TEM: Transmission electron microscopy; IHC: Immunohistochemistry; dpi: Days post inoculated; FVR: Feline viral rhinotracheitis; URTD: Upper respiratory tract disease; HE: Haematoxylin and eosin; TG: Trigeminal ganglia; CCG: Ciliary ganglia; WBC: White blood cells; LYM: Lymphocyte; SAA: Serum amyloid A; MOI: Multiplicity of infection; CPE: Cytopathic effect; MEM: Minimum essential medium; ULN: Upper limits of normal; AI: Artificial inoculated; NJ: Neighbor-joining.

## Declarations

### Acknowledgements

We would like to thank the staff at the Yueli pet clinic, Beiyuan pet clinic in Changchun and Jilin for sample collection. In addition, we also would like to thank the veterinarians at Jau Wellhope Veterinary Teching Hospital for the complete blood count and SAA analysis.

### Authors' contributions

Conceptualization, GXH and SSY; methodology, JTN, HZ, DB, QZ, KW and HLH; software, SZ and YLZ; validation, HD, JZW and FXM; formal analysis, JTN; investigation, JTN, HZ and SSY; writing-original draft

preparation, JTN and SSY; writing-review and editing, SSY and GXH; visualization, HD; project administration, GXH; funding acquisition, GXH. All authors have read and agreed to the published version of the manuscript.


### Funding

This research was funded by the Research Project of the National Key Research and Development Plan of China (Grant no. 2016YFD0501002).


### Availability of data and materials

The data generated and/or analyzed during this study are available from the corresponding author upon request. The sequences of genome of FHV-1 CH-B isolated in the present study was available in the Genbank (Accession number: MT813047).

### Ethics approval and consent to participate

All animal experiments in the present study were performed with the approval from the Animal care committee of Jilin Agricultural University, Jilin Province, China.

### Consent for publication

Not applicable.

### Competing Interests

'Competing Interests' The authors declare no conflict of interest.

## References


1. Gaskell R, Dawson S, Radford A, Thiry E. Feline herpesvirus. Vet Res. 2007;38:337–54. http://doi:10.1051/vetres:2006063.
2. Maes R Felid herpesvirus type 1 infection in cats: a natural host model for alphaherpesvirus pathogenesis. *ISRN Vet Sci* 2012, 2012, 495830. [3671728] http://doi:10.5402/2012/495830.
3. Thiry E, Addie D, Belak S, Boucraut-Baralon C, Egberink H, Frymus T, Gruffydd-Jones T, Hartmann K, Hosie MJ, Lloret A, Lutz H, Marsilio F, Pennisi MG, Radford AD, Truyen U, Horzinek MC. Feline herpesvirus infection. ABCD guidelines on prevention and management. J Feline Med Surg. 2009;11:547–55. http://doi:10.1016/j.jfms.2009.05.003. [7129359].
4. Maggs DJ. Update on pathogenesis, diagnosis, and treatment of feline herpesvirus type 1. Clin Tech Small Anim Pract. 2005;20:94–101. http://doi:10.1053/j.ctsap.2004.12.013.
5. Lomonte P, Herpesvirus Latency. On the Importance of Positioning Oneself. Adv Anat Embryol Cell Biol. 2017;223:95–117. http://doi:10.1007/978-3-319-53168-7_5.

6. Gould D. Feline herpesvirus-1: ocular manifestations, diagnosis and treatment options. J Feline Med Surg. 2011;13:333–46. http://doi:10.1016/j.jfms.2011.03.010.
7. Monne Rodriguez JM, Leeming G, Kohler K, Kipar A. Feline Herpesvirus Pneumonia: Investigations Into the Pathogenesis. Vet Pathol. 2017;54:922–32. http://doi:10.1177/0300985817720982.
8. Dowers KL, Hawley JR, Brewer MM, Morris AK, Radecki SV, Lappin MR. Association of Bartonella species, feline calicivirus, and feline herpesvirus 1 infection with gingivostomatitis in cats. J Feline Med Surg. 2010;12:314–21. http://doi:10.1016/j.jfms.2009.10.007.
9. Sun HT, Li YG, Jiao WY, Liu CF, Liu XJ, Wang HJ, Hua FY, Dong JX, Fan ST, Yu ZJ, Gao YW, Xia XZ. Isolation and Identification of Feline Herpesvirus Type 1 from a South China Tiger in China. Viruses 2014, 6, 1004–14. http://doi:10.3390/v6031004.
10. Witte CL, Lamberski N, Rideout BA, Vaida F, Citino SB, Barrie MT, Haefele HJ, Junge RE, Murray S, Hungerford LL. Epidemiology of clinical feline herpesvirus infection in zoo-housed cheetahs (Acinonyx jubatus). Javma-J Am Vet Med A. 2017;251:946–56. http://doi:10.2460/javma.251.8.946.
11. Batista HBDR, Vicentini FK, Franco AC, Spilki FR, Silva JCR, Adania CH, Roehe PM. Neutralizing antibodies against feline herpesvirus type 1 in captive wild felids of Brazil. J Zoo Wildlife Med. 2005;36:447–50. http://doi:10.1638/04-060.1.
12. Maggs DJ. Antiviral Therapy for Feline Herpesvirus Infections. Vet Clin N Am-Small. 2010;40:1055–7. http://doi:10.1016/j.cvsm.2010.07.010.
13. Thomasy SM, Maggs DJ. A review of antiviral drugs and other compounds with activity against feline herpesvirus type 1. Vet Ophthalmol. 2016;19:119–30. http://doi:10.1111/vop.12375.
14. Quimby J, Lappin M. Feline focus: Update on feline upper respiratory diseases: condition-specific recommendations. Compend Contin Educ Vet. 2010;32:E1–10. http://www.ncbi.nlm.nih.gov/pubmed/20473846.
15. Stiles J. Ocular manifestations of feline viral diseases. Vet J 2014, 201, 166–73. [7110540] http://doi:10.1016/j.tvjl.2013.11.018.
16. Lewin AC, Kolb AW, McLellan GJ, Bentley E, Bernard KA, Newbury SP, Brandt CR, Genomic. Recombinational and Phylogenetic Characterization of Global Feline Herpesvirus 1 Isolates. Virology. 2018;518:385–97. http://doi:10.1016/j.virol.2018.03.018. [5935452].
17. Bol S, Bunnik EM. Lysine supplementation is not effective for the prevention or treatment of feline herpesvirus 1 infection in cats: a systematic review. BMC Vet Res. 2015;11:284. http://doi:10.1186/s12917-015-0594-3. [4647294].
18. Hoover EA, Griesemer RA. Experimental feline herpesvirus infection in the pregnant cat. Am J Pathol. 1971;65:173–88. http://www.ncbi.nlm.nih.gov/pubmed/4328861. [2047512].
19. Hamano M, Maeda K, Mizukoshi F, Une Y, Mochizuki M, Tohya Y, Akashi H, Kai K. Experimental infection of recent field isolates of feline herpesvirus type 1. J Vet Med Sci. 2003;65:939–43. http://doi:10.1292/jvms.65.939.
20. Townsend WM, Jacobi S, Tai SH, Kiupel M, Wise AG, Maes RK. Ocular and neural distribution of feline herpesvirus-1 during active and latent experimental infection in cats. Bmc Vet Res. 2013;9:185.

http://doi:10.1186/1746-6148-9-185.

21. Sack GH. Jr. Serum Amyloid A (SAA) Proteins. Subcell Biochem. 2020;94:421–36. http://doi:10.1007/978-3-030-41769-7_17.
22. Pennington MR, Ledbetter EC, Van de Walle GR. New Paradigms for the Study of Ocular Alphaherpesvirus Infections: Insights into the Use of Non-Traditional Host Model Systems. Viruses. 2017;9:349–71. http://doi:10.3390/v9110349. [5707556].
23. Sykes JE, Allen JL, Studdert VP, Browning GF. Detection of feline calicivirus, feline herpesvirus 1 and Chlamydia psittaci mucosal swabs by multiplex RT-PCR/PCR. Vet Microbiol. 2001;81:95–108. http://doi:10.1016/s0378-1135(01)00340-6.
24. Tian J, Liu D, Liu Y, Wu H, Jiang Y, Zu S, Liu C, Sun X, Liu J, Qu L. Molecular characterization of a feline calicivirus isolated from tiger and its pathogenesis in cats. Vet Microbiol. 2016;192:110–7. http://doi:10.1016/j.vetmic.2016.07.005.

# Figures

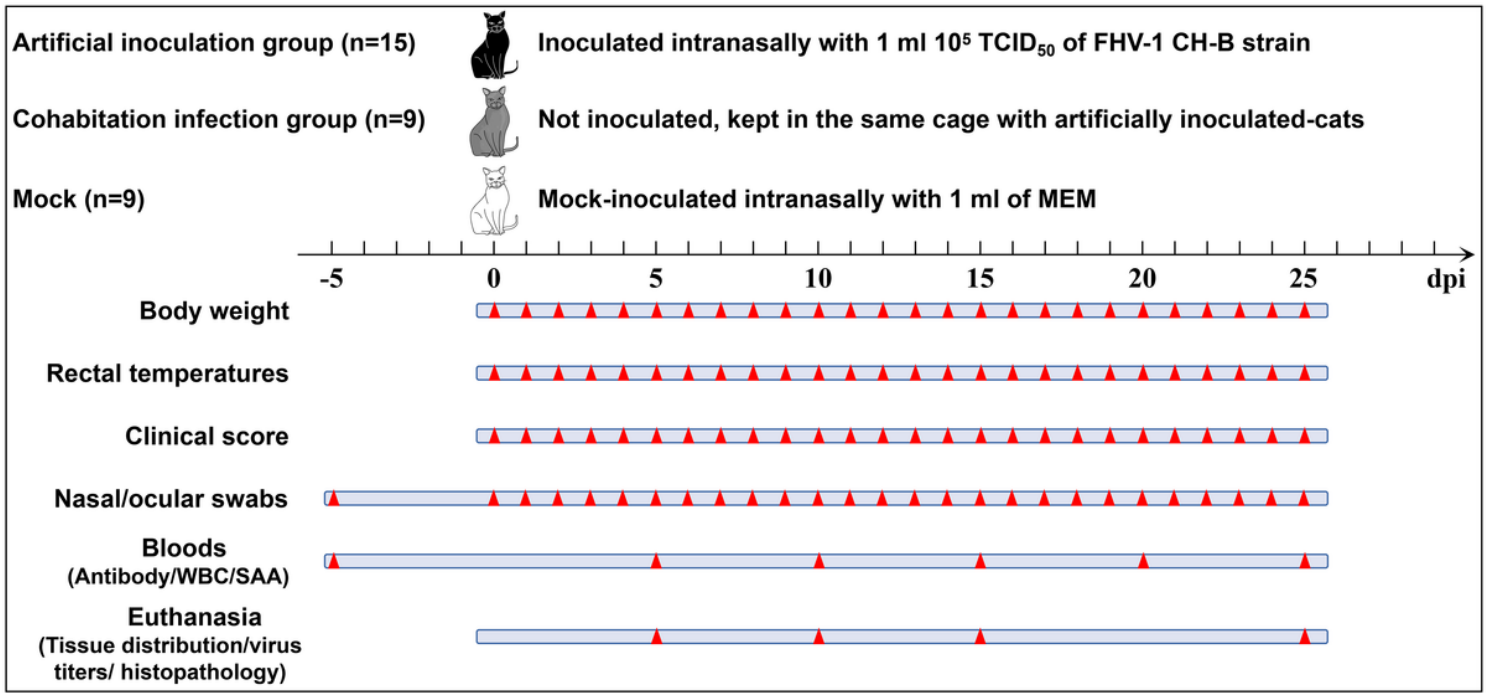


**Figure 1**

Experimental design of FHV-1 infection model and the collection of clinical indicators or samples.

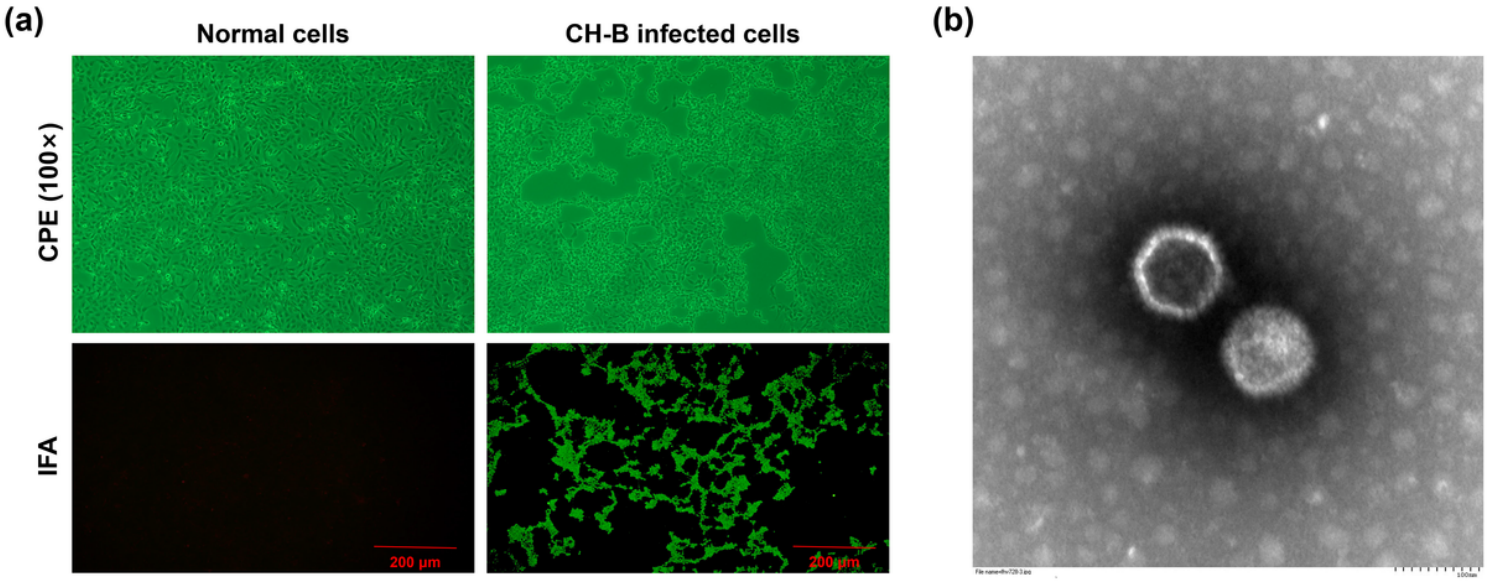


## Figure 2

Virus isolation and identification of FHV-1 CH-B through IFA and TEM. (a) The cytopathic effect (CPE) and IFA identification. The CPE, characterized by cell rouding, pyknosis and focal-like forms, were observed in F81cells inoculated with FHV-1 CH-B strain at 60 h post-inoculation. Green fluorescence represents the FHV-1 antigen within infected cells. (b) Negative-stained transmission electron microscopy of FHV-1 CH-B particles. Spherical viruses with diameters ranging from 120-160 nm were observed in cell cultures.

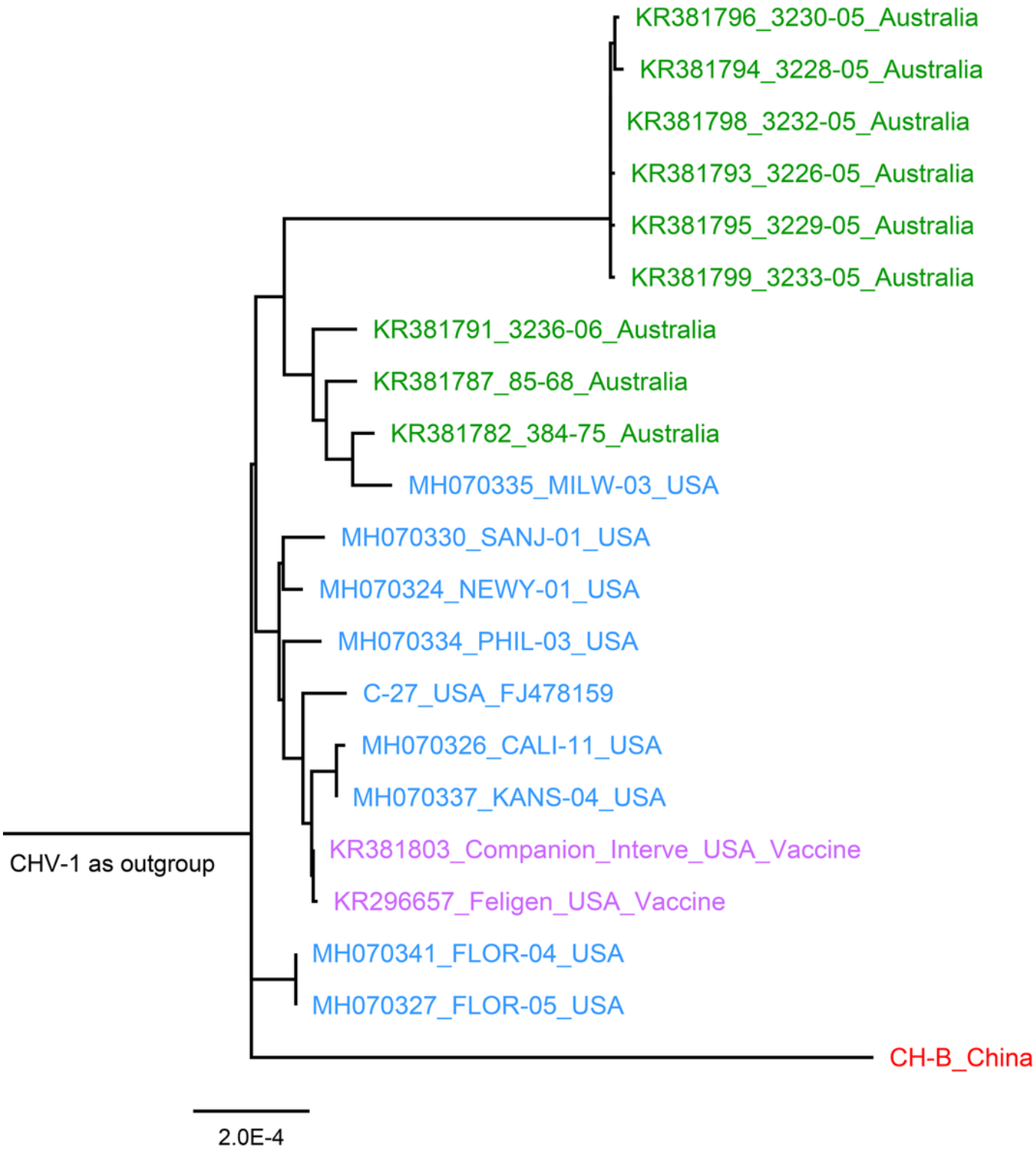


**Figure 3**

Neighbor-joining tree constructed based on the complete genome nucleotide sequences of isolate CH-B and 20 reference FHV-1 strain. Isolates of FHV-1 isolated from USA, Australia and China are shown in blue, green and red, respectively, the FHV-1 vaccine isolates are shown in purple. The tree is generated using the Kimura 2-parameter model and 500 bootstrap replicates with MEGA 7.0.

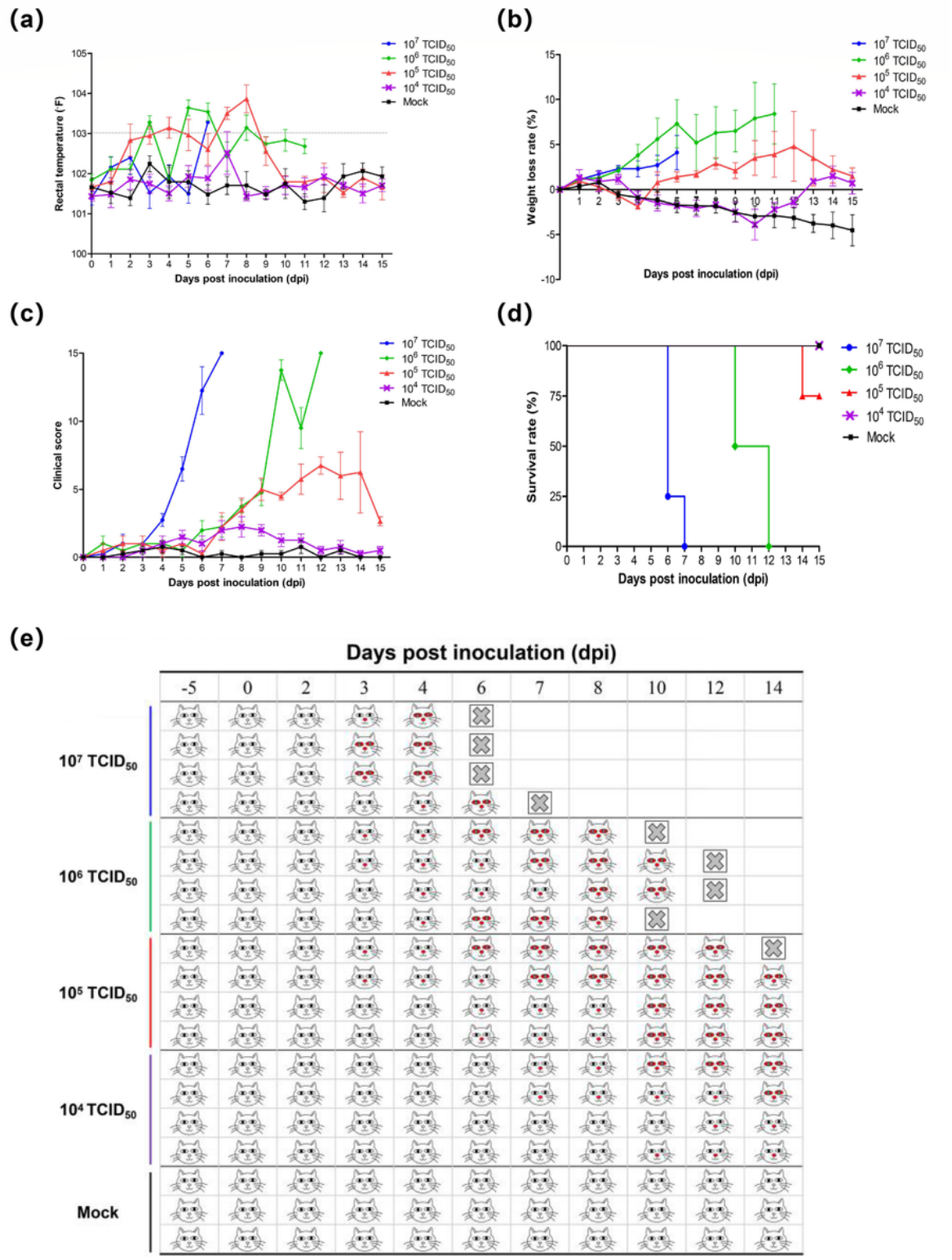


## Figure 4

Rectal temperature (a), body weight loss rate (c), clinical score (b), survival rate (d) and nasal/ocular virus shedding of cats challenged with different doses of FHV-1 CH-B strain. Group A, B, C and D (n=4) were inoculated intranasally with 107, 106, 105 or 104 TCID50 of FHV-1 CH-B strain, respectively. Group E (n=3) was mock-inoculated with MEM. Nasal and ocular virus shedding were determined by the detection

of FHV-1 DNA in nasal and ocular swabs daily. Red noses or eyes indicated that the nasal or ocular swab was tested to be positive for FHV-1, cross in box indicate that this cat have died.

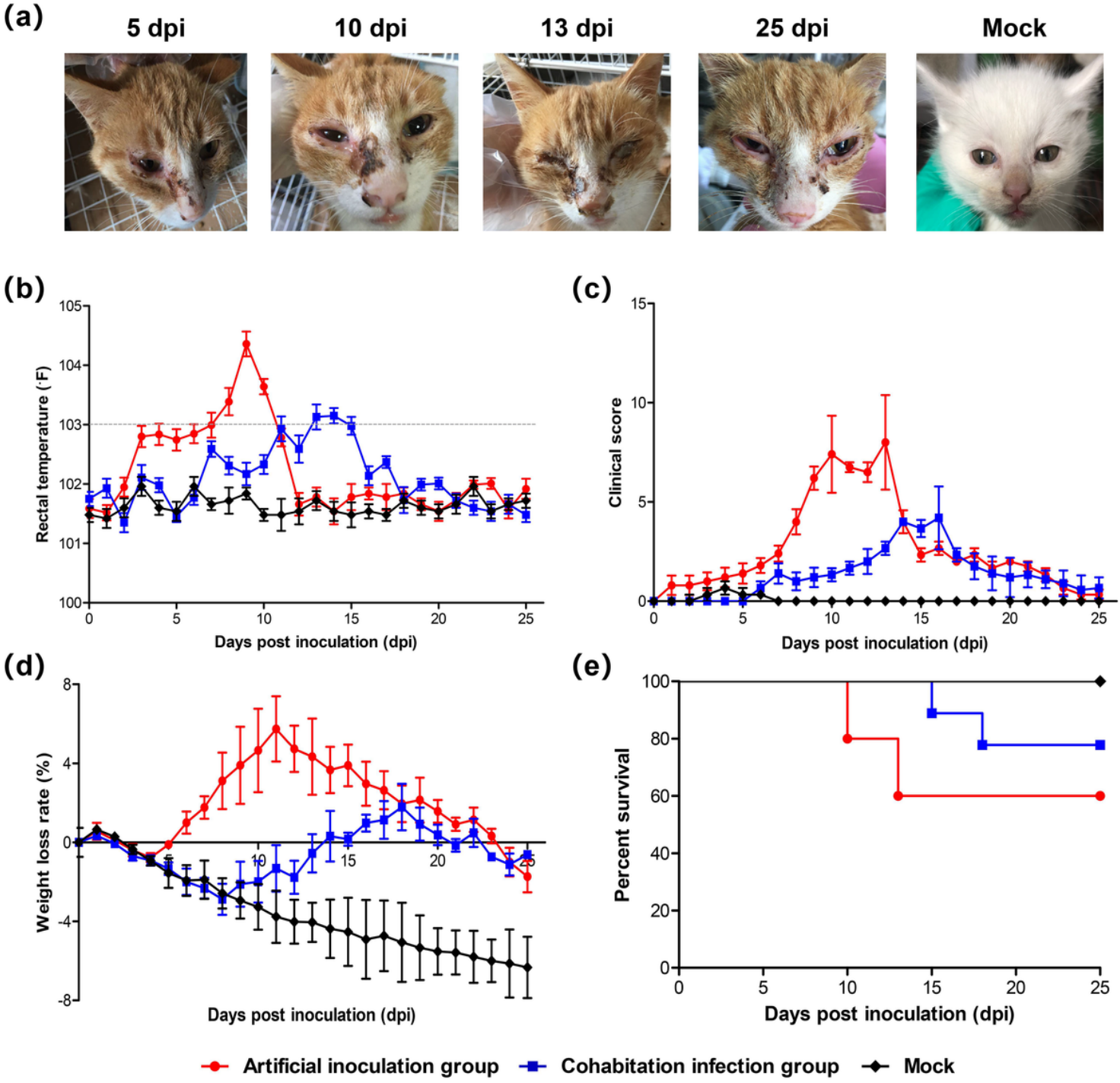


## Figure 5

Clinical feature (a), rectal temperature (b), clinical score (c), body weight loss rate (d) and survival rate (e) of artificially inoculated cats (challenged with 105 TCID50 of FHV-1 CH-B strain), cohabitation infected cats and mocks. (a) Clinical features of a artificially inoculated cat at 5, 10, 13 and 25 dpi, respectively.

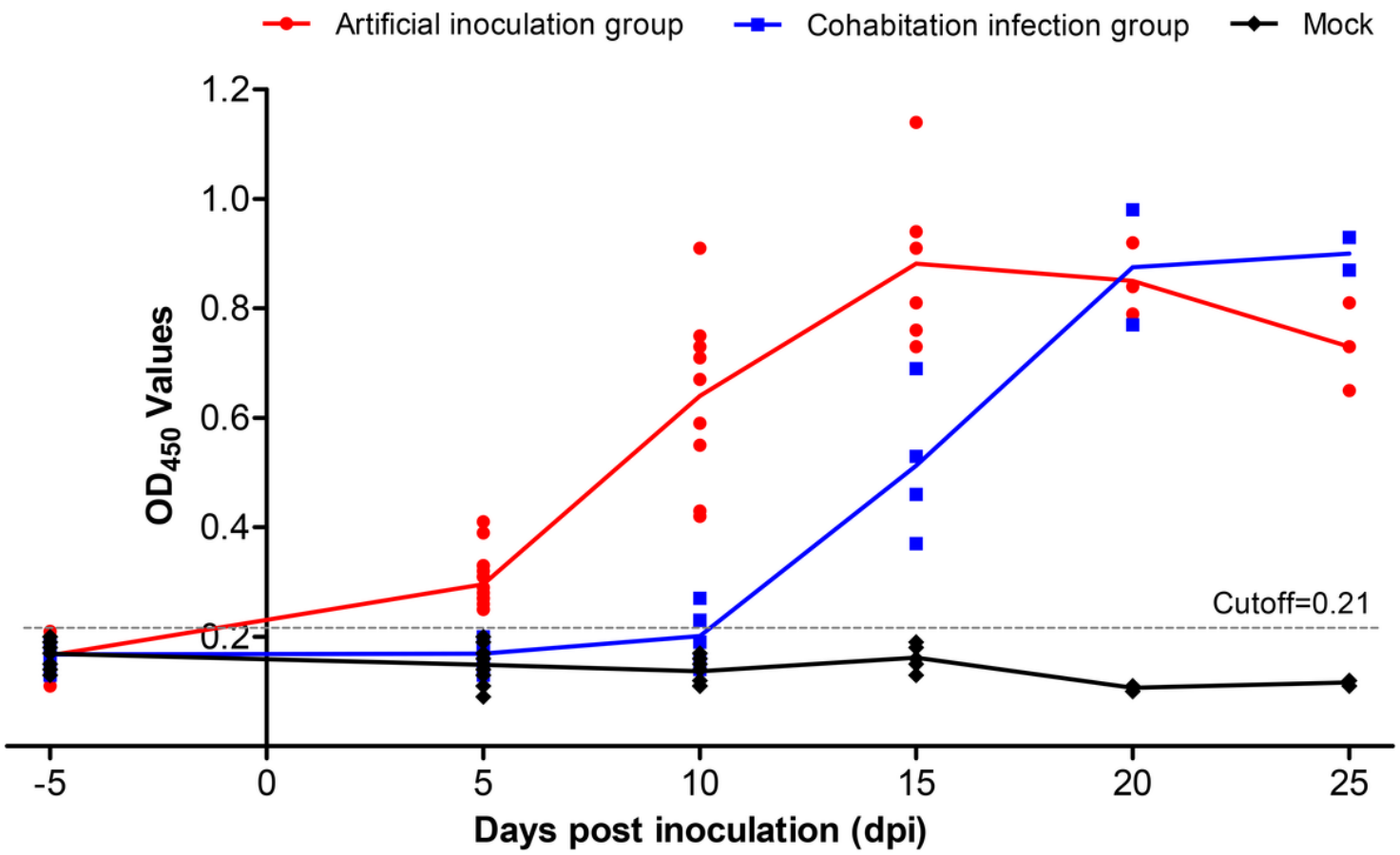


**Figure 6**

Time course of seroconversion in cats of each group. Antibodies against FHV-1 in serum were tested using an commercial ELISA kit, and antibody titres are represented by ELISA absorbance (OD450 nm values).

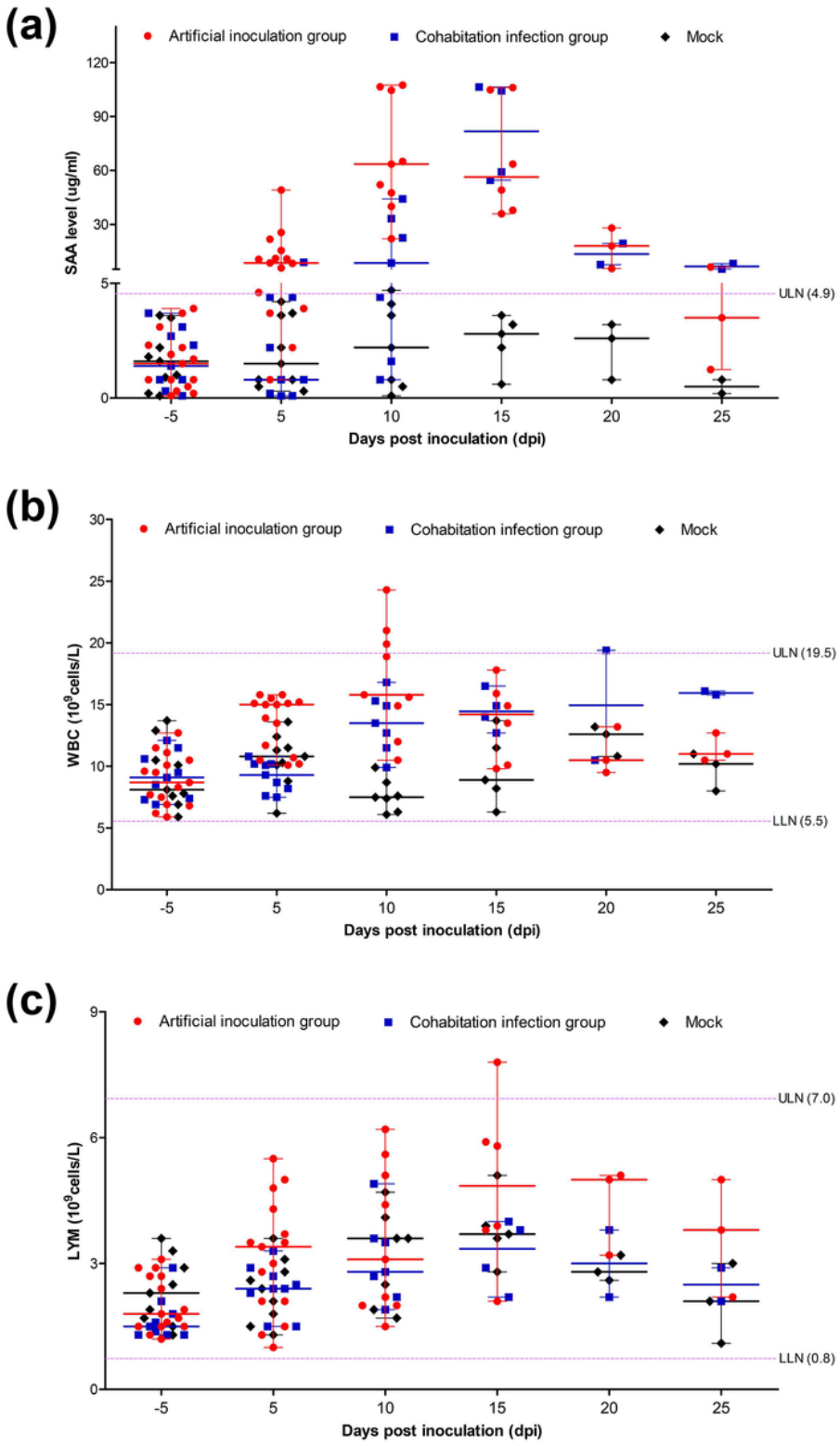


## Figure 7

Serum amyloid A (SAA) contents (a), white blood cells counts (b) and lymphocyte counts (c) in all cats of each group at each of time point. ULN, upper limits of normal; LLN, lower limits of normal.

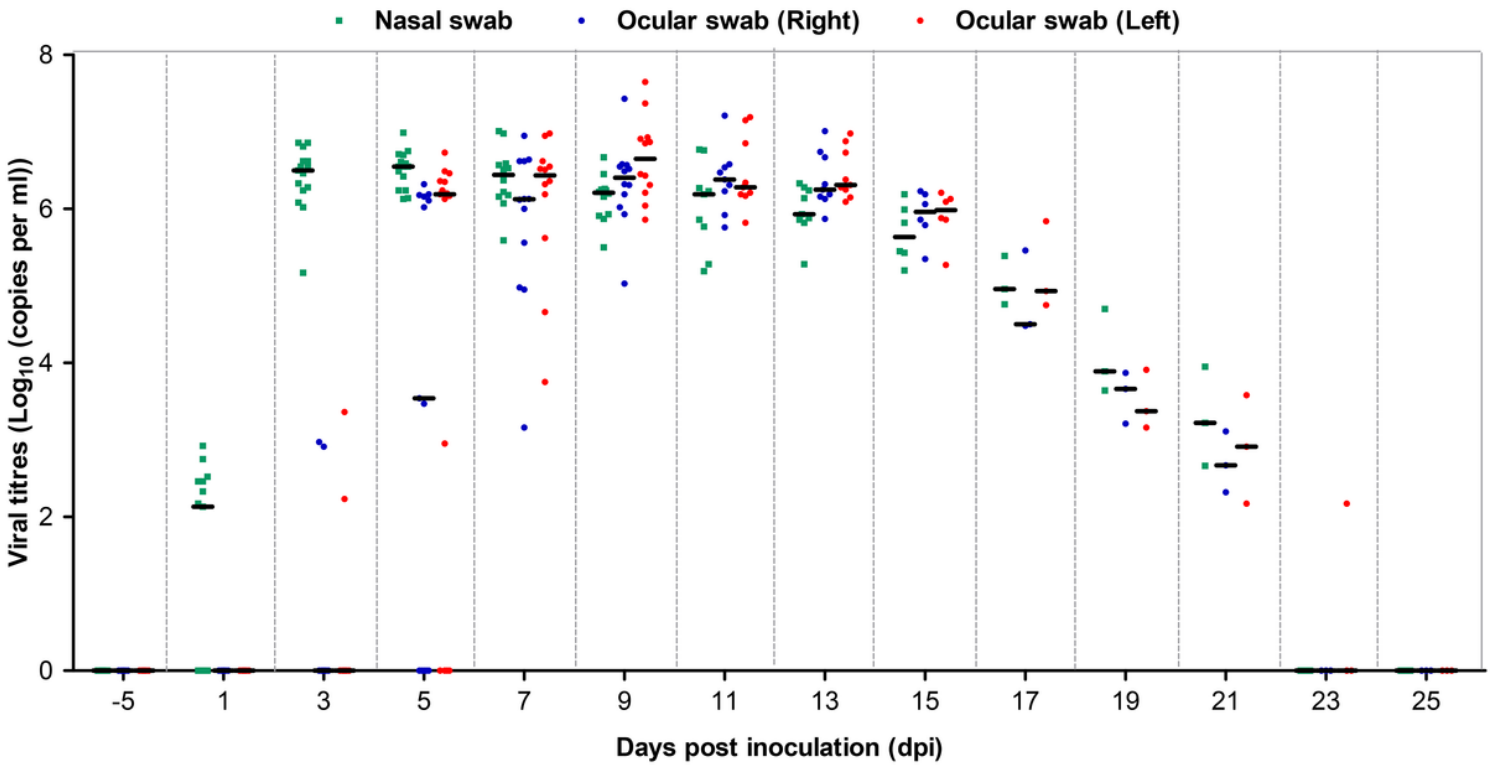


## Figure 8

Virus shedding and viral loads in nasal and ocular swabs from FHV-1 artificial infected cats.

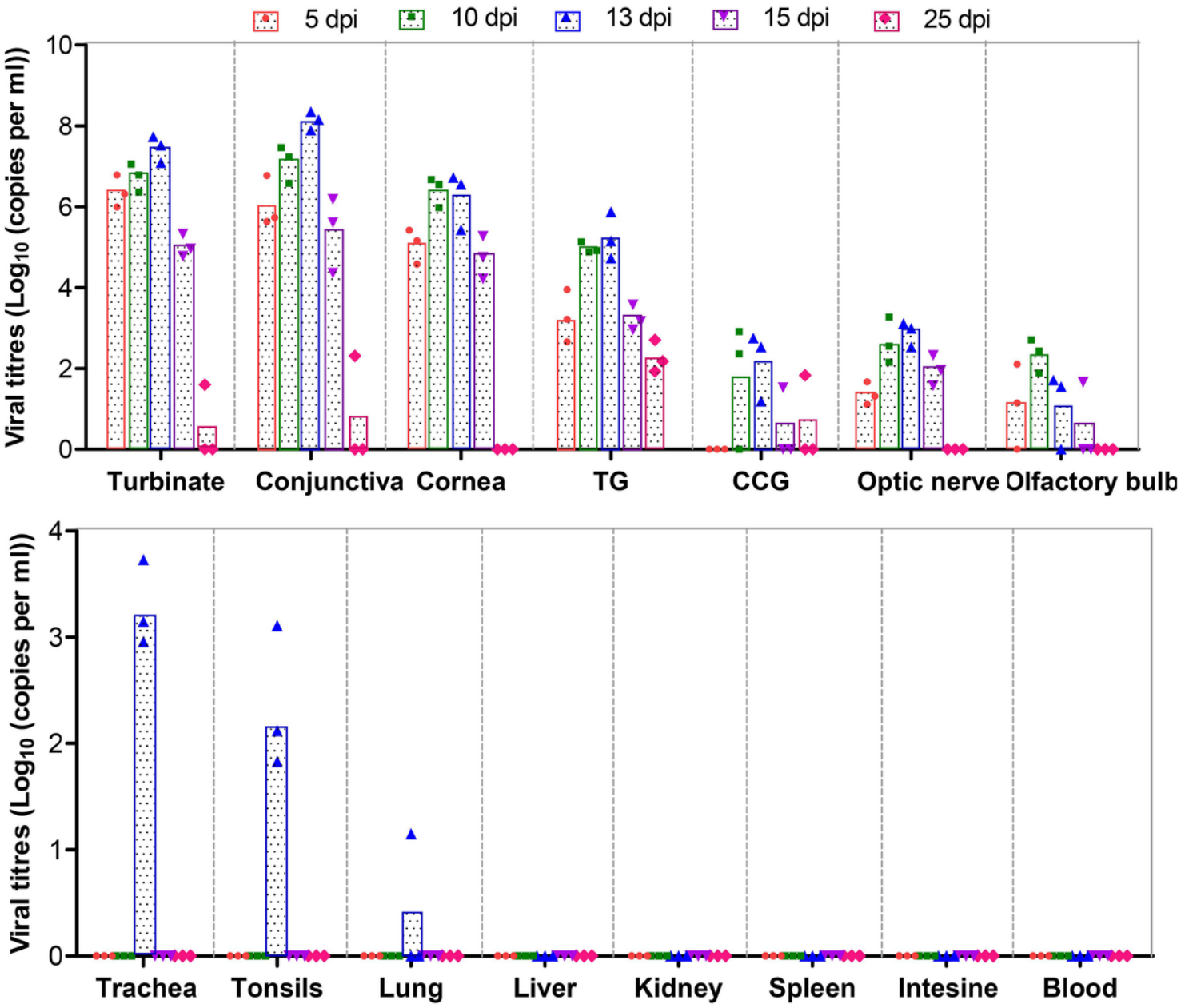


## Figure 9

Viral DNA distribution and viral titres in tissues from FHV-1 artificial infected cats.

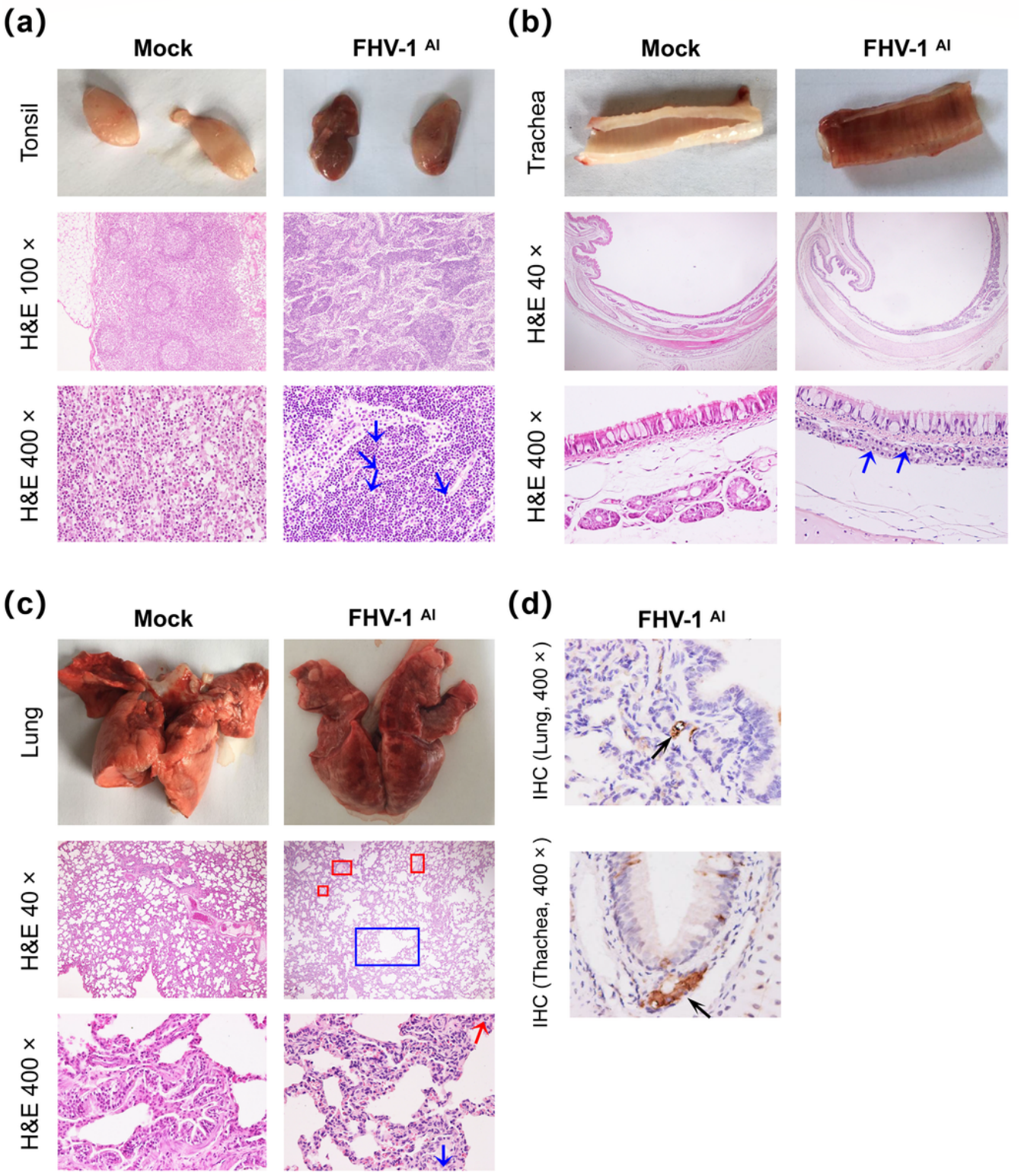


**Figure 10**

Gross pathology, histopathology and IHC of the tonsil (a), trachea (b, d) and lungs (c, d) in FHV-1 artificial infected cats. Tonsil, trachea and lungs were collected from artificial infected cats died at days 13 post inoculated due to infection and uninfected control cats euthanized at 15 dpi.

# Supplementary Files

This is a list of supplementary files associated with this preprint. Click to download.

- ARRIVEChecklist.pdf
- Supplementarymaterials.pdf